Interplay of Charge Transfer, Dimensionality, and Amide Hydrogen Bond Network Adaptability in TCNQF$_4$ Complexes of EDO-TTF-CONH$_2$ and EDT-TTF-CONH$_2$

Stéphane A. Baudron,* Cécile Mézière,* Karine Heuzé,† Marc Fourmigué,* Patrick Batail,*,[1]
Philippe Molinié,† and Pascale Auban-Senzier‡

*Chimie Inorganique, Matériaux et Interfaces, FRE 2447 CNRS-Université d'Angers, Bâtiment K, UFR Sciences, 2, Boulevard Lavoisier, F-49045 Angers, France; †Institut Jean Rouxel, 2, rue de la Houssinière, 44322 Nantes, France; and ‡Laboratoire de Physique des Solides, Bât 510, UMR CNRS-Université Paris-Sud, F-91405 Orsay, France

[EDO-TTF-CONH$_2$][TCNQF$_4$], triclinic system, space group *P*-1, *a* = 8.2479(12) Å, *b* = 12.282(2) Å, *c* = 12.6842(18) Å, α = 113.850(17)°, β = 106.420(17)°, γ = 90.284(19)°, *V* = 1116.8(4) Å^3; and [EDT-TTF-CONH$_2$]$_2$[TCNQF$_4$], triclinic system, space group *P*-1, *a* = 6.5858(9) Å, *b* = 11.699(2) Å, *c* = 12.2281(18) Å, α = 104.000(19)°, β = 93.611(17)°, γ = 98.279(19)°, *V* = 899.9(3) Å^3, whose π-donor molecules, (ethylenedioxo)-carbamoyltetrathiafulvalene and (ethylenedithio)-carbamoyltetrathiafulvalene, respectively, differ solely by the nature of the chalcogen atoms in their outer ethylene dichalcogeno bridge, yet form very different charge-transfer complexes with the same π-acceptor. [EDO-TTF-CONH$_2$$^{\bullet+}$]$_2$[TCNQF$_4$$^{\bullet-}$]$_2$ is a diamagnetic insulating ionic salt with a three-dimensional rock-salt-type structure based on discrete dimers while in the semi-conducting mixed-valence complex, [EDT-TTF-CONH$_2$]$_2$$^{\bullet+}$[TCNQF$_4$$^{\bullet-}$], the mixed-valence dimers aggregate into infinite chains interspersed within parallel rows of non-interacting radical anions. It is shown how the robust and adaptable supramolecular amide hydrogen bond tweezers-like motifs common to the two solids simply comply to the 3-to-1 dimensionality reduction upon substitution of O for S. © 2002 Elsevier Science (USA)

Key Words: charge-transfer salts; crystal engineering; hydrogen bonding; tetrathiafulvalene.

1. INTRODUCTION

Changing the nature of the chalcogen atoms in TTF derivatives with the perspective to modify their intermolecular HOMO–HOMO interaction energies is a strategy which has essentially concerned substitutions of sulfur for selenium and tellurium. Substitution of sulfur for oxygen

only concerns those chalcogen atoms outer to the TTF core and had been demonstrated by the synthesis of BEDO-TTF (1) and recently EDO-TTF (2,3), the oxo analogs of BEDT-TTF (4) and EDT-TTF (5) (Scheme 1). As nicely highlighted by Zorina *et al.* (6), BEDO-TTF salts are not isostructural with their BEDT-TTF analogs. Furthermore, radical cation salts of BEDT-TTF and BEDO-TTF with the same anion have very often different stoichiometries. In order to design and eventually control the patterns of intermolecular interactions in these molecular materials, another complementary approach is to make use of weak intermolecular interactions such as hydrogen (7) or halogen bonding (8), thus creating situations where the latter will compete with the former manipulation of intermolecular p_π–p_π overlap interactions (9). This is exemplified by the series [EDT-TTF-Br$_2$]$_2$$^{\bullet+}I_3^-$ (10) and [EDO-TTF-Br$_2$]$_3$$^{\bullet+}I_3^-$ (11) where different stoichiometries and crystal structures are associated with different supramolecular Br···I interaction networks. However, to our knowledge, no studies have been performed on how the chalcogen modification and the functionalization of TTF derivatives interplay. This may be achieved by comparing the salts of functionalized EDT-TTF and EDO-TTF with the same anion. In the case of hydrogen bonding, the recent syntheses of the primary and secondary amide series, EDT-TTF-CONR_1R_2 (12) and EDO-TTF-CONR_1R_2 ($R_{1,2} = H$, Me) (3), make the comparison accessible.

Our first attempts to electrocrystallize EDO-TTF-CONR_1R_2 revealed that their salts are typically more soluble than EDT-TTF-CONR_1R_2 salts (9, 13) to the point that no crystals could be obtained yet by this method (14). In this paper, we describe the preparation and structural characterization of charge-transfer complexes of the primary amides EDO-TTF-CONH$_2$ and EDT-TTF-CONH$_2$, prepared by chemical oxidation by the strong
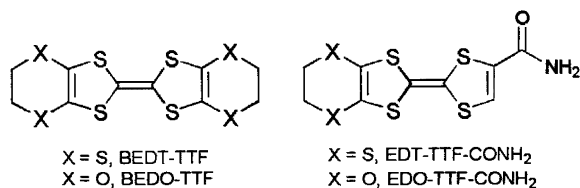
SCHEME 1

π-acceptor TCNQF$_4$, and discuss the interplay of factors which are responsible for their strikingly different stoichiometries and electronic properties upon the substitution of sulfur for oxygen in the ethylenedichalcogeno bridge.

2. EXPERIMENTAL

2.1. Syntheses

EDO-TTF-CONH$_2$ and EDT-TTF-CONH$_2$ were prepared as described previously (3, 12). The stoichiometry of both salts was first determined by EMPA on the precipitates obtained by reacting a 1/1 mixture of each donor with TCNQF$_4$ as follows:

(EDO-TTF-CONH$_2$)(TCNQF$_4$). Addition of TCNQF$_4$ (18 mg, 0.065 mmol) in THF (10 mL) to a solution of EDO-TTF-CONH$_2$ (20 mg, 0.065 mmol) in THF causes a color change from orange to brown. The mixture is left at 4°C overnight to afford shiny purple platelets (24 mg, 63%) suitable for X-ray. Calc. for C$_{21}$H$_7$N$_5$O$_3$F$_4$S$_4$: C, 43.37; H, 1.21; N, 12.04; found C, 43.22; H, 1.27; N, 11.91. IR (KBr): 2176, 2196 cm^{-1} (CN).

(EDT-TTF-CONH$_2$)$_2$(TCNQF$_4$). To a solution of EDT-TTF-CONH$_2$ (20 mg, 0.06 mmol) in THF (30 mL), TCNQF$_4$ (8.2 mg, 0.03 mmol) in THF (10 mL) is added. The solution then turns from yellow to dark brown. The mixture is left at 4°C for 24 h affording black platelets (21 mg, 75%) recovered by filtration. Calc. for C$_{30}$H$_{14}$N$_6$O$_2$F$_4$S$_{12}$: C, 37.88; H, 1.48; N, 8.83; found C, 37.83 ; H, 1.49; N, 8.62. IR (KBr): 2172, 2194 cm^{-1} (CN). A single crystal suitable for X-ray diffraction was obtained by slow diffusion of the THF solutions of the donor and acceptor in dichloromethane in a U-shaped cell.

2.2. X-Ray Crystallography

Data collection conditions and structure refinement details are collected in Table 1. Data were collected on a Stoe-IPDS diffractometer at 293 K. Structures were solved using SHELXS-86 and refined by the full-matrix least-squares method on F^2, using SHELXL-93 (G. M. Sheldrick, University of Göttingen, 1993) with anisotropic thermal parameters for all non-hydrogen atoms. The hydrogen atoms were introduced at calculated positions and not refined (riding model). ORTEP representations and numbering schemes for both structures are presented in Fig. 1. Crystallographic data (excluding structure factors) for the structures reported in this paper have been deposited with the Cambridge Crystallographic Data Centre as supplementary publication no. CCDC-186488/ 186489. Copies of the data can be obtained free of charge on application to CCDC, 12 Union Road, Cambridge CB2 1EZ, UK (Fax: 44 1223 336-033; E-mail: deposit@ccdc. cam.ac.uk).

2.3. Magnetic Measurements

Magnetic susceptibility data were collected on a Quantum Design MPMS5 SQUID magnetometer at 5000 Gauss with polycrystalline samples of [EDO-TTF-CONH$_2$] [TCNQF$_4$] (20.27 mg) and [EDT-TTF-CONH$_2$]$_2$[TCNQF$_4$] (20.83 mg). The data were corrected for molecular diamagnetism and sample holder contributions.

3. RESULTS AND DISCUSSION

3.1. Ionic Salt vs Mixed-Valence Complex

When engaged in charge-transfer complexes with the strong π-acceptor TCNQF$_4$ ($E_{red} = 0.53$ V/SCE in CH$_3$CN), EDO-TTF-CONH$_2$ ($E_{ox} = 0.40$ V/SCE in CH$_3$CN), easier to oxidize than EDT-TTF-CONH$_2$ ($E_{ox} = 0.50$ V/SCE in CH$_3$CN), is more likely to form a fully charge transferred salt ($\Delta E = 0.13$ V) than the latter. In addition, given the near match of the redox potentials of
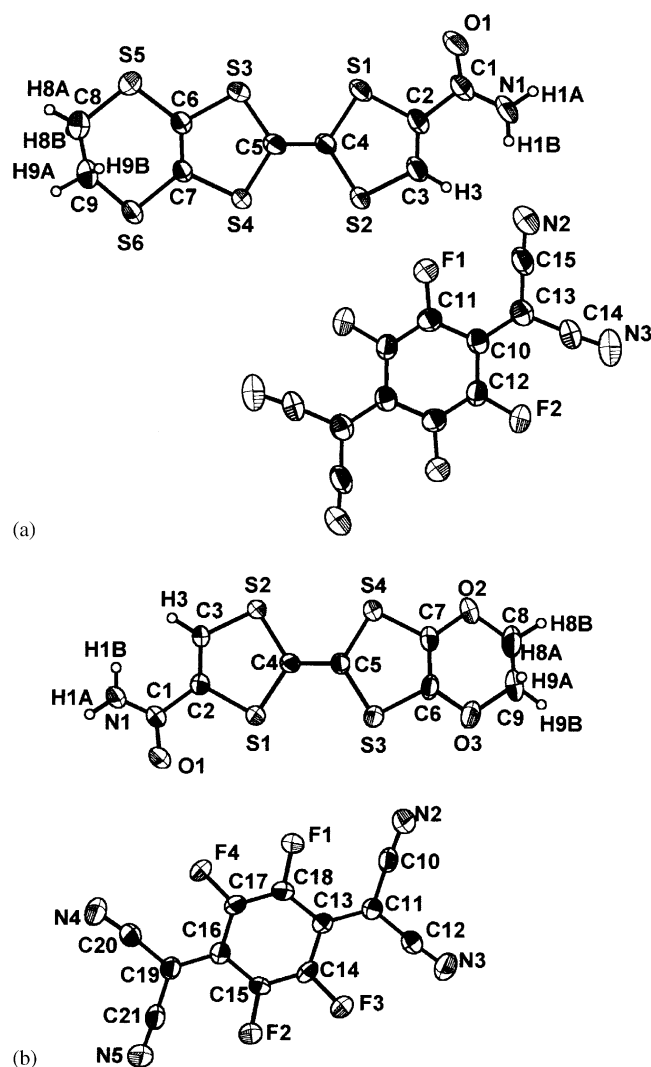
TABLE 1
Crystallographic Data

	[EDT-TTF-CONH$_2$]$_2$ [TCNQF$_4$]	[EDO-TTF-CONH$_2$] [TCNQF$_4$]
Formula	C$_{30}$H$_{14}$N$_6$O$_2$F$_4$S$_{12}$	C$_{21}$H$_7$N$_5$O$_3$F$_4$S$_4$
Formula mass	951.31	581.60
Temperature (K)	293 (2)	293 (2)
Crystal system	Triclinic	Triclinic
Space group	P-1	P-1
a (Å)	6.5858(9)	8.2479(12)
b (Å)	11.699(2)	12.282(2)
c (Å)	12.2281(18)	12.6842(18)
α (deg)	104.000(19)	113.850(17)
β (deg)	93.611(17)	106.420(17)
γ (deg)	98.279(19)	90.284(19)
V (Å^3)	899.9(3)	1116.8(4)
Z	1	2
d_{calc} (g cm^{-3})	1.755	1.730
μ (mm^{-1})	0.792	0.497
Reflections collected	8806	11 127
Independent reflections	3250	4025
R_{int}	0.057	0.053
R_1 [$I > 2\sigma(I)$]	0.0321 [1906]	0.0319 [2036]
wR_2	0.0624	0.0503

(a)

(b)

FIG. 1. ORTEP representations and atom numbering schemes for the structures of (a) [EDT-TTF-CONH$_2$]$_2$[TCNQF$_4$] and (b) [EDO-TTF-CONH$_2$] [TCNQF$_4$] (ellipsoids are drawn at 50% probability level).

EDT-TTF-CONH$_2$ and TCNQF$_4$ ($\Delta E = 0.03$ V), a mixed-valence complex is expected in this case. The observed stoichiometries of the compounds, 1:1 in [EDO-TTF-CONH$_2$][TCNQF$_4$] and 2:1 in [EDT-TTF-CONH$_2$]$_2$[TCNQF$_4$], are consistent with these expectations. The analysis of the molecular structures in the crystals (Tables 2 and 3), indeed confirms that [EDO-TTF-CONH$_2^{\bullet+}$][TCNQF$_4^{\bullet-}$] is an ionic salt with fully oxidized ions and [EDO-TTF-CONH$_2$]$_2^{\bullet+}$ [TCNQF$_4^{\bullet-}$], a mixed-valence complex, hence their respective formulations.

3.2. Dimensionality Reduction

[EDO-TTF-CONH$_2$][TCNQF$_4$] crystallizes in the triclinic system, space group P-1. The unit cell contains one π-donor and one molecule of TCNQF$_4$, both in the general position (Fig. 1b). In the crystal structure (Fig. 2), both molecules form discrete centrosymmetric dimers (Fig. 3) and any [EDO-TTF-CONH$_2^{\bullet+}$]$_2$ ion sees six [TCNQF$_4^{\bullet-}$]$_2$ nearest neighbors of opposite charge and vice versa, with essentially no interaction between like dimers. Thus, [EDO-TTF-CONH$_2^{\bullet+}$]$_2$[TCNQF$_4^{\bullet-}$]$_2$ can be viewed as a fully ionic, three-dimensional rock salt analog. In [EDO-TTF-CONH$_2^{\bullet+}$]$_2$, the radical cations adopt a somewhat eclipsed pattern of intradimer overlap (Figs. 3c and 3d) with a short plane-to-plane distance of 3.374(2) Å, typical of a fully oxidized, discrete diamagnetic dimer configuration (15). Likewise, within [TCNQF$_4^{\bullet-}$]$_2$ dimers, the radical anions are essentially eclipsed with a short interplanar distance of 3.154(3) Å.

[EDT-TTF-CONH$_2$]$_2$[TCNQF$_4$] crystallizes in the triclinic system, space group P-1. The unit cell contains one π-donor in the general position and one half-molecule of TCNQF$_4$ on an inversion center (Fig. 1a). Bond length analysis for EDT-TTF-CONH$_2$ (Table 2) and TCNQF$_4$

TABLE 2
Bond Lengths (Å) in EDO-TTF-CONH$_2$ ($X = $ O) and EDT-TTF-CONH$_2$ ($X = $ S) in Their Neutral and Oxidized Forms

	EDT-TTF-CONH$_2^a$	[EDO-TTF-CONH$_2$][TCNQF$_4$]	EDTTTFCONH$_2^{1/2+\ b}$	[EDT-TTF-CONH$_2$]$_2$ [TCNQF$_4$]
a	1.32(3)	1.387(3)	1.371(9)	1.372(3)
b	1.77(2)	1.724(3)	1.723(8)	1.739(3)
c	1.76(2)	1.730(3)	1.748(8)	1.743(3)
d	1.75(2)	1.715(3)	1.752(8)	1.729(3)
e	1.75(2)	1.723(3)	1.733(8)	1.737(3)

^{a} From Ref. (12).

^{b} In (EDT-TTF-CONH$_2$)$_6$AsF$_6$ (9).

TABLE 3
Bond Lengths (Å) in TCNQF$_4$ and Nitrile Frequencies in the Two Salts and Some Reference Compounds
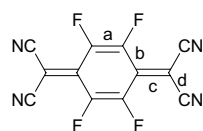
	TCNQF$_4$	[EDO-TTF-CONH$_2$][TCNQF$_4$]	[EDT-TTF-CONH$_2$]$_2$[TCNQF$_4$]	TCNQF$_4^{\bullet-}$ [a]	TCNQF$_4^{2-}$ [b]
a	1.335	1.352(4)	1.360(4)	1.36	1.373
b	1.439	1.411(4)	1.410(4)	1.42	1.398
c	1.373	1.410(4)	1.416(4)	1.42	1.457
d	1.440	1.423(5)	1.423(5)	1.435	1.403
C≡N	1.142	1.145(5)	1.137(5)	1.14	1.154
ν_{CN}	2215, 2230	2176, 2196	2172, 2194	2179, 2195	2133, 2167
Ref.	(16)	This work	This work	(17)	(18)

[a] In [FeCp$_2$][TCNQF$_4$].
[b] In [FeCp$_2$]$_2$[TCNQF$_4$].

(Table 3) (16–18) indicates that the complex can be formulated as [EDT-TTF-CONH$_2$]$_2^{\bullet+}$[TCNQF$_4^{\bullet-}$]. The charge on the TCNQF$_4$ is further confirmed by the value of its nitrile stretching frequency (Table 3). Within the mixed-valence dimers [EDT-TTF-CONH$_2$]$_2^{\bullet+}$, the molecules adopt a slipped, bond-over-ring type of conformation (Figs. 3a and 3b) with a plane-to-plane distance of 3.457(2) Å, typically longer than in
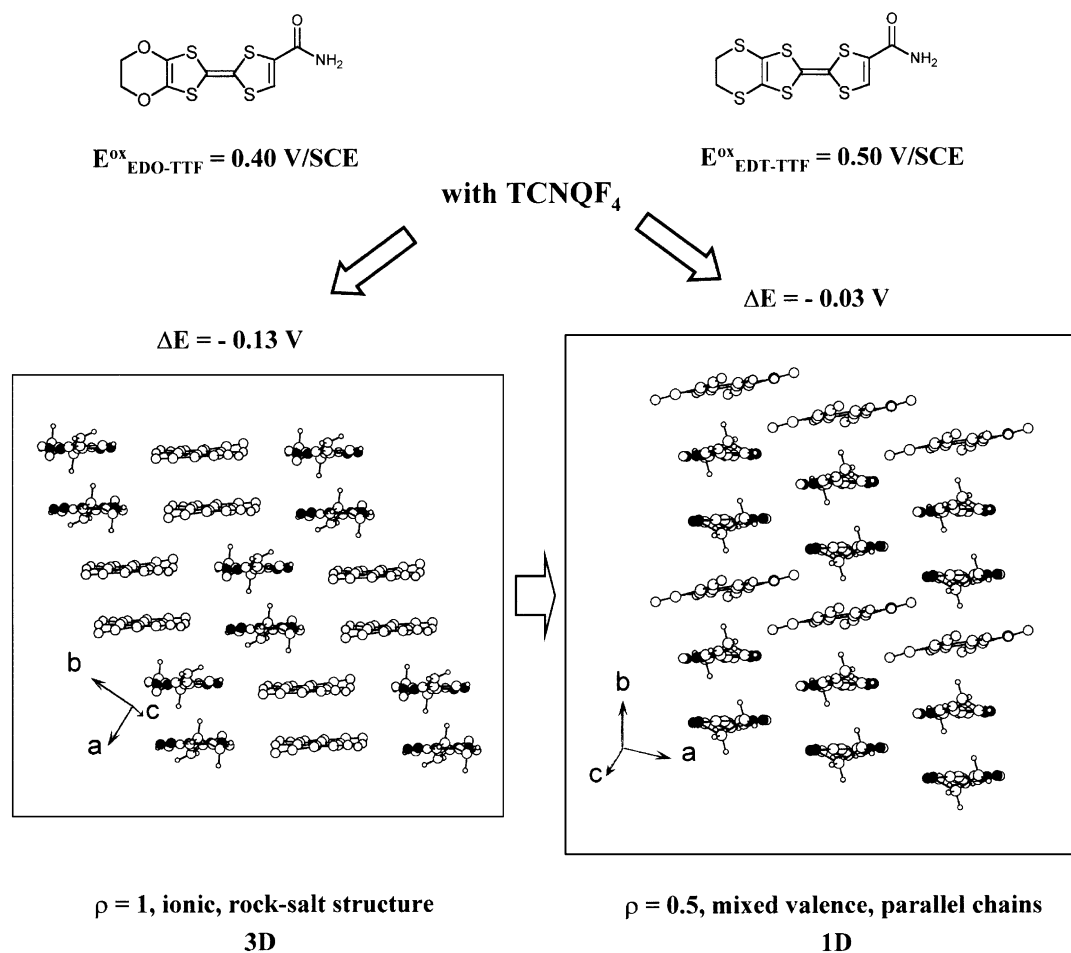

FIG. 2. An overview of the thermodynamic and structural features of [EDO-TTF-CONH$_2^{\bullet+}$]$_2$[TCNQF$_4^{\bullet-}$]$_2$ (left-hand side) and [EDT-TTF-CONH$_2$]$_2^{\bullet+}$[TCNQF$_4^{\bullet-}$] (right-hand side). The structures are viewed down the π-donor long molecular axis.
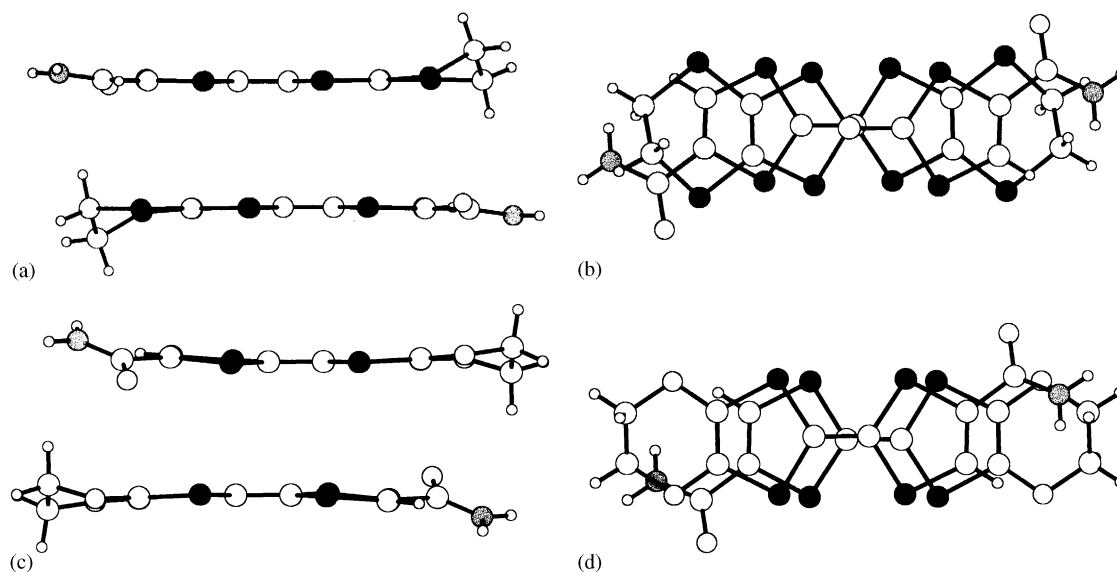
FIG. 3. (a) and (b) Intradimer pattern of overlap in $[EDT\text{-}TTF\text{-}CONH_2]_2^{\bullet+}$; (c) and (d) intradimer pattern of overlap in $[EDO\text{-}TTF\text{-}CONH_2^{\bullet+}]_2$.

$[EDO\text{-}TTF\text{-}CONH_2^{\bullet+}]_2$, as expected. The most salient consequence of the stabilization of a mixed-valence configuration of the π-donor dimers is perhaps, by comparison to the former ionic rock-salt solid, the profound reconstruction of the overall architecture to form one-dimensional chains, $\{[EDT\text{-}TTF\text{-}CONH]_2^{\bullet+}\}_\infty^1$, where the mixed-valence dimers aggregate and overlap along their transverse direction, as shown in Fig. 2. These discrete chains of dimers run parallel to discrete chains of essentially non-interacting $TCNQF_4^{\bullet-}$ molecules.

3.3. Adaptability of the Supramolecular Pattern of the Amide Hydrogen Bond Tweezers

As exemplified in Fig. 4, the robust, recurrent centrosymmetric cyclic hydrogen bond $R_2^2(8)$ (19) dimer motif, common to a great many primary amides (20, 21) including neutral EDT-TTF-CONH$_2$ (12), is identified in both $[EDO\text{-}TTF\text{-}CONH_2^{\bullet+}]_2[TCNQF_4^{\bullet-}]_2$ and $[EDT\text{-}TTF\text{-}CONH_2]_2^{\bullet+}[TCNQF_4^{\bullet-}]$. Comparing the supramolecular hydrogen patterns shown in Fig. 4 and whose geometrical characteristics are given in Table 4, one discloses the remarkable adaptability of the precise intermolecular, robust tweezers-like hydrogen bond motif identified previously in $[EDT\text{-}TTF\text{-}CONH_2]_6[AsF_6]$ (9) and $[EDT\text{-}TTF\text{-}CONHMe]_2[Cl \cdot H_2O]$ (13), where the remaining amide N–H hydrogen bond donor and the adjacent, hydrogen bond donor vinylic C–H of the TTF core cooperate and reach out differently towards the nitrile hydrogen bond acceptors of TCNQF$_4$.

Consider first the pattern for $[EDO\text{-}TTF\text{-}CONH_2^{\bullet+}]_2$ $[TCNQF_4^{\bullet-}]_2$ in Fig. 4b. Here, the amide functionalities and the TTF cores rotate away from each other by $\pm 23.6(2)^\circ$ across the centrosymmetric dimer motif in such a way that any pair of hydrogen bond tweezers grasp two nitrile acceptors of two TCNQF$_4$'s pertaining to the same dimer. In $[EDT\text{-}TTF\text{-}CONH_2]_2^{\bullet+}[TCNQF_4^{\bullet-}]$ (Fig. 4a), the amide functionalities and the TTF cores remain coplanar since it is necessary for any pair of tweezers to capture one nitrile of one single TCNQF$_4$ only. The latter resulting cyclic motif is then $R_2^1(7)$ as already encountered in radical cation salts of EDT-TTF-CONH$_2$ (13).

Note that in both $[EDO\text{-}TTF\text{-}CONH_2^{\bullet+}]_2[TCNQF_4^{\bullet-}]_2$ and $[EDO\text{-}TTF\text{-}CONH_2]_2^{\bullet+}[TCNQF_4^{\bullet-}]$, the hydrogen bond network also includes a weak ethylenic C–H$\cdots$NC interaction ((sp^3)–C$_9$–H$_{9B}\cdots$N$_2$ and (sp^3)–C$_8$–H$_{8A}\cdots$N$_3$, respectively, Table 4), a likely explanation of the absence of disorder of the flexible ethylene dioxo and ethylene dithio bridges in the solids.

3.4. Magnetic and Electronic Properties

In the case of $[EDT\text{-}TTF\text{-}CONH_2]_2^{\bullet+}[TCNQF_4^{\bullet-}]$, the 2:1 stoichiometry and the mixed-valence character lead to the possibility of conductivity in this salt. Extended Hückel calculations is a valuable method to evaluate the HOMO$\cdots$HOMO overlap interaction in such systems (22). The main interaction is found within $[EDT\text{-}TTF\text{-}CONH_2]_2^{\bullet+}$ dimers ($\beta_{intra} = 0.45$ eV). These dimers are only weakly coupled (Fig. 2) along a ($\beta_{inter} = 0.05$ and 0.02 eV). As a consequence, the possibility of metallic conductivity is ruled out. This is confirmed by single-crystal conductivity measurement revealing a semi-conducting behavior with a room-temperature conductivity of 3×10^{-3} S cm^{-1}. The magnetic susceptibility of $[EDT\text{-}TTF\text{-}CONH_2]_2^{\bullet+}[TCNQF_4^{\bullet-}]$ (Fig. 5) exhibits a
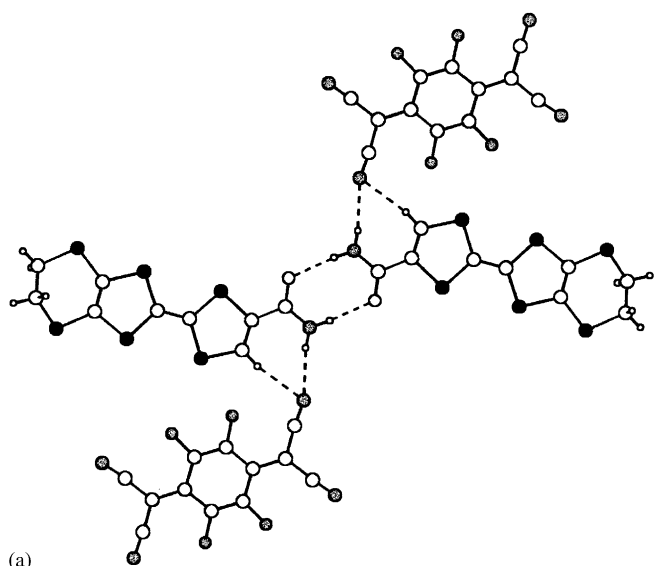
(a)
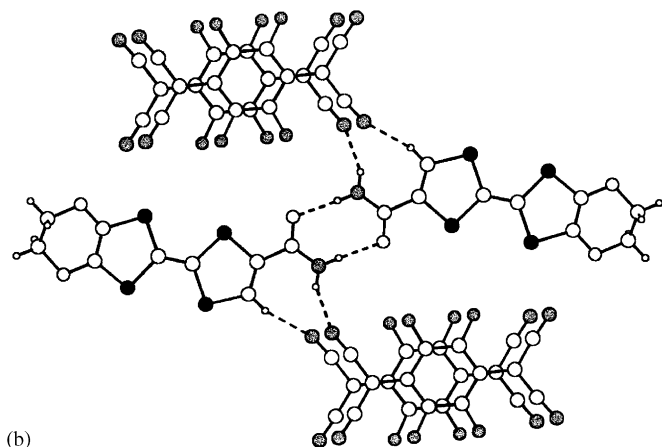
(b)

FIG. 4. Illustration of the common, R$_2^2$(8) cyclic dimer hydrogen bond pattern and different intermolecular hydrogen bond tweezers expression in (a) [EDT-TTF-CONH$_2$]$_2$[TCNQF$_4$] and (b) [EDO-TTF-CONH$_2$]$_2$ [TCNQF$_4$]$_2$.

TABLE 4
Geometrical Characteristics of the Hydrogen Bonds in the Two Salts

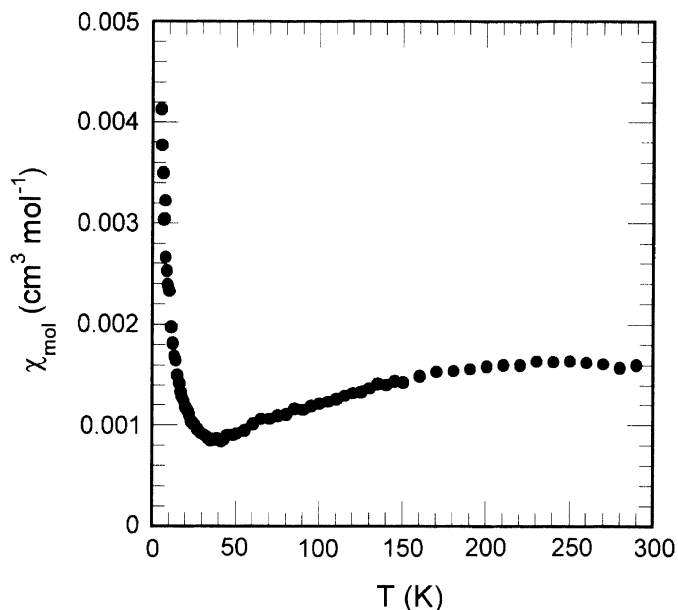|	D···A (Å)	H···A (Å)	α(D–H···A) (deg)
[EDT-TTF-CONH$_2$]$_2$ [TCNQF$_4$]			
N$_1$–H$_{1A}$···O$_1$	2.915(3)	2.057	174.2
N$_1$-H$_{1B}$···N$_2$	3.132(4)	2.306	160.8
(sp^2)–C$_3$–H$_3$···N$_2$	3.405(5)	2.587	147.1
(sp^3)–C$_8$–H$_{8A}$···N$_3$	3.329(4)	2.421	155.6
[EDO-TTF-CONH$_2$] [TCNQF$_4$]			
N$_1$–H$_{1A}$···O$_1$	2.891(3)	2.066	160.4
N$_1$-H$_{1B}$···N$_3$	3.083(4)	2.035	150.7
(sp^2)–C$_3$–H$_3$···N$_4$	3.318(3)	2.461	153.3
(sp^3)–C$_9$–H$_{9B}$···N$_2$	3.306(4)	2.599	129.9

FIG. 5. Temperature dependence of the magnetic susceptibility in [EDT-TTF-CONH$_2$]$_2$[TCNQF$_4$].

weakly temperature-dependent paramagnetism compatible with the semi-conducting character of the salt, albeit the absence of contribution of the almost isolated [TCNQF$_4$]$^{-\bullet}$ anions to the susceptibility is not clear at this stage of the work. Preliminary EPR experiments performed on a polycrystalline sample of [EDT-TTF-CONH$_2$]$_2^{\bullet+}$[TCNQF$_4^{\bullet-}$] at room temperature show the presence of a single broadened line which can be decomposed as the sum of two components, one at $g = 2.0048$ with $\Delta H = 4\,G$ and another at $g = 2.0070$ with $\Delta H = 5\,G$. Based on analogous TTF and TCNQ derivatives (23), the former can be tentatively attributed to the [TCNQF$_4^{\bullet-}$] moieties while the latter is attributed to the [EDT-TTF-CONH$_2$]$_2^{+\bullet}$ dimers.

On the other hand, [EDT-TTF-CONH$_2^{\bullet+}$]$_2$[TCNQF$_4^{\bullet-}$]$_2$ is diamagnetic in the whole temperature range explored. This is well correlated with the strong intradimer interaction within both [EDO-TTF-CONH$_2^{\bullet+}$]$_2$ and [TCNQF$_4^{\bullet-}$]$_2^-$ dimers. Indeed, the intradimer HOMO···HOMO interaction in $(2)_2^{2+}$ amounts to 0.92 eV while it is only 0.21 eV for the interdimer interaction. In the case of [TCNQF$_4^{\bullet-}$]$_2$, the intra- and interdimer interactions amount to 1.11 and 0.04 eV, respectively.

4. CONCLUSION

We have described the synthesis, crystal structures, conducting and magnetic properties of [EDO-TTF-CONH$_2^{\bullet+}$]$_2$[TCNQF$_4^{\bullet-}$]$_2$ and [EDT-TTF-CONH$_2$]$_2^{\bullet+}$ [TCNQF$_4^{\bullet-}$], two new charge-transfer salts between primary amide-functionalized π-donors and TCNQF$_4$ shown

to exhibit different stoichiometries and degrees of charge transfer. The salient manifestation of the substitution of sulfur for oxygen in the outer ethylenedichalcogeno bridges of the π-donor molecules is to favor the stabilization of a 2:1 mixed-valence complex with TCNQF$_4$, a consequence of the higher oxidation potential (by 0.1 V) of the sulfur analog and of its near match with the reduction potential of TCNQF$_4$ ($\Delta E = 0.03$ V). The change from a full charge-transfer to a mixed-valence configuration imposes a profound reconstruction of the overall architecture of the 1:1 ionic rock-salt solid to form one-dimensional $\{[\text{EDT-TTF-CONH}_2]_2^{\bullet+}\}_\infty^1$ chains, where the mixed-valence dimers aggregate and overlap along their transverse direction. Remarkably, the supramolecular amide hydrogen bond tweezers-like motifs common to the two solids, simply comply to the dimensionality reduction by capturing one nitrile of one single TCNQF$_4$ only per pair of hydrogen bond tweezers in [EDO-TTF-CONH$_2]_2^{\bullet+}$ [TCNQF$_4^{\bullet-}$] instead of two pertaining to the same TCNQF$_4$ dimer in the three-dimensional ionic solid [EDO-TTF-CONH$_2^{\bullet+}]_2$[TCNQF$_4^{\bullet-}]_2$. This nicely illustrates both the robustness and adaptability of hydrogen bond motifs in redox-amide-based systems and confirms their usefulness as supramolecular construction elements in TTF-based materials.

[EDO-TTF-CONH$_2^{\bullet+}]_2$[TCNQF$_4^{\bullet-}]_2$ and [EDO-TTF-CONH$_2]_2^{\bullet+}$[TCNQF$_4^{\bullet-}$], having different stoichiometries and crystal structures, have different electronic properties. The former is insulating and diamagnetic while [EDO-TTF-CONH$_2]_2^{\bullet+}$[TCNQF$_4^{\bullet-}$] exhibit a sizeable conductivity at room temperature (3×10^{-3} S cm^{-1}). The semi-conducting $\{[\text{EDT-TTF-CONH}_2]_2^{\bullet+}\}_\infty^1$ chains are interspersed amongst essentially non-interacting TCNQF$_4^{\bullet-}$ anion radicals. The system exhibits a single composite electron spin resonance of the radical cation and anion spins at room temperature.

ACKNOWLEDGMENTS

REFERENCES

1. T. Suzuki, H. Yamochi, G. Srdanov, K. Hincelman, and F. Wudl, *J. Am. Chem. Soc.* **111,** 3108 (1989).

2. G. C. Papavassiliou, V. C. Kakoussis, D. J. Lagouvardos, and G. A. Mousdis, *Mol. Cryst. Liq. Cryst.* **181,** 171 (1990); T. Mori, H. Inokuchi, and A. M. Kini, *Chem. Lett.* 1279 (1990).

3. C. Mézière, M. Fourmigué, and J.-M. Fabre, *C. R. Acad. Sci. IIc* **3,** 387 (2000).

4. M. Mizuno, A. F. Garito, and M. P. Cava, *J. Chem. Soc. Chem. Commun.* 18 (1978).

5. G. C. Papavassiliou, G. A. Mousdis, J. S. Zambounis, A. Terzis, A. Hountas, B. Hilti, C. W. Mayer, and J. Pfeiffer, *Synth. Met.* **B379,** 27 (1988); M. Fourmigué, F. C. Krebs, and J. Larsen, *Synthesis* (1993) 509.

6. L. V. Zorina, S. S. Khasanov, R. P. Shibaeva, M. Gener, R. Rousseau, E. Canadell, L. A. Kushch, E. B. Yagubskii, O. O. Drozdova, and K. Yakushi, *J. Mater. Chem.* **10,** 2017 (2000).

7. P. Blanchard, K. Boubekeur, M. Sallé, G. Duguay, M. Jubault, A. Gorgues, J. D. Martin, E. Canadell, P. Auban-Senzier, D. Jérome, and P. Batail, *Adv. Mater.* **4,** 579 (1992); A. J. Moore, M. R. Bryce, A. S. Batsanov, J. N. Heaton, C. W. Lehmann, J. A. K. Howard, N. Robertson, A. E. Underhill, and I. F. Perepichka, *J. Mater. Chem.* **8,** 1541 (1998); O. Neilands, S. Belyakov, V. Tilika, and A. Edzina, *J. Chem. Soc. Chem. Comm.* 325 (1995); A. Dolbecq, M. Fourmigué, F. C. Krebs, P. Batail, E. Canadell, R. Clérac, and C. Coulon, *Chem. Eur. J* **2,** 1275 (1996); G. Ono, H. Tera, S. Higuchi, T. Sugawara, A. Izuoka, and T. Mochida, *J. Mater. Chem.* **10,** 2277 (2000); J.-P. Legros, F. Dahan, L. Binet, C. Carcel, and J.-M. Fabre, *J. Mater. Chem.* **10,** 2685 (2000).

8. S. L. Price, A. J. Stone, J. Lucas, R. S. Rowland, and A. E. Thornley, *J. Am. Chem. Soc.* **116,** 4910 (1994); G. R. Desiraju and R. Parthasarathy, *J. Am. Chem. Soc.* **111,** 8725 (1989).

9. K. Heuzé, M. Fourmigué, P. Batail, E. Canadell, and P. Auban-Senzier, *Chem. Eur. J* **5,** 2971 (1999).

10. B. Domercq, T. Devic, M. Fourmigué, P. Auban-Senzier, and E. Canadell, *J. Mater. Chem.* **11,** 1570 (2001).

11. M. Iyoda, E. Ogura, T. Takano, K. Hara, Y. Kuwatani, T. Kato, N. Yoneyama, J. Nishijo, A. Miyazaki, and T. Enoki, *Chem. Lett.* 680 (2000).

12. K. Heuzé, M. Fourmigué, and P. Batail, *J. Mater. Chem.* **9,** 2373 (1999).

13. K. Heuzé, C. Mézière, M. Fourmigué, P. Batail, C. Coulon, E. Canadell, P. Auban-Senzier, and D. Jérome, *Chem. Mater.* **12,** 1898 (2000).

14. P. Batail, K. Boubekeur, M. Fourmigué, and J.-C. P. Gabriel, *Chem. Mater.* **10,** 3005 (1998).

15. See for example: T. Devic, J. N. Bertran, B. Domercq, E. Canadell, N. Avarvari, P. Auban-Senzier, and M. Fourmigué, *New J. Chem.* **25,** 1418 (2001).

16. T. J. Emge, M. Maxfield, D. O. Cowan, and T. J. Kirstenmacher, *Mol. Cryst. Liq. Cryst.* **65,** 161 (1981).

17. J. S. Miller, J. H. Zhang, and W. M. Reiff, *Inorg. Chem.* **26,** 600 (1987).

18. D. A. Dixon, J. C. Calabrere, and J. S. Miller, *J. Phys. Chem.* **93,** 2284 (1989).

19. M. Etter, *Acc. Chem. Res.* **23,** 120 (1990).

20. L. Leiserowitz and A. T. Hagler, *Proc. R. Soc. Lond. A* **388,** 133 (1983).

21. F. H. Allen, W. D. Motherwell, P. R. Raithby, G. P. Shields, and R. Taylor, *New J. Chem.* **1,** 25 (1999).

22. M. H. Whangbo, J. M. Williams, P. C. W. Leung, M. A. Beno, T. J. Emge, and H. H. Wang, *Inorg. Chem.* **24,** 3500 (1985).

23. A. Dolbecq, M. Fourmigué, P. Batail, and C. Coulon, *Chem. Mater.* **6,** 1413 (1994).